

# 转子物性对超临界汽轮机启动热应力的影响

刘彦丰, 郝润田, 高建强, 赵军友

(华北电力大学 能源与动力工程学院, 河北 保定 071003)

**摘要:** 汽轮机转子材料多采用 30CrMoV 低碳合金钢, 其物性参数随温度变化显著。所建转子热应力计算模型, 考虑了转子材料物性随温度变化的影响。通过仿真试验, 分析了国产某 600 MW 超临界汽轮机冷态、温态、热态和极热态 4 种启动工况下转子热应力的变化趋势, 并与常物性转子热应力模型的计算结果进行了比较。结果表明: 转子材料物性参数随温度的变化显著影响其启动热应力的大小, 为提高汽轮机转子热应力在线监测模型的计算精度提供有益参考。

**关键词:** 汽轮机转子; 物性; 热应力; 模型

中图分类号: TK124; TK262      文献标识码: A

## 引 言

超临界机组是未来我国火力发电机组的发展趋势。由于超临界机组的蒸汽参数较亚临界高得多, 尽管两者使用的材料相同或基本相近, 但服役条件却更为恶劣。而其汽轮机转子在运行过程中受机组频繁启停、负荷变动的影 响, 其转子金属内部经常产生较大的温度梯度, 并由此而产生交变的热应力, 严重削弱着机组寿命, 成为火电机组寿命最薄弱的环节。因此准确掌握机组转子的热应力水平, 特别是超临界机组转子的热应力水平显得十分重要。

汽轮机转子材料多为 30CrMoV 低碳合金钢, 其各项物理性质均随温度变化显著(如: 密度  $\rho$ 、比热  $c$ 、导热系数  $\lambda$ 、弹性模量  $E$ 、线性膨胀系数  $\beta$ 、泊桑数  $\nu$  等)<sup>[3,6~7]</sup>。而这些物性参数涉及整个热应力的计算过程, 因此在计算中计入材料的物性变化是十分必要的。而很多转子热应力计算模型为了更易于实现在线监测, 将物性简化为常物性<sup>[1~2,9]</sup>, 这样必然与实际结果产生偏差。本文则采用克兰克-尼科尔森有限差分计算模型, 在计算中充分考虑了转子材料的物性随温度变化的影响, 对国产 600 MW 超临界汽轮机转子在冷态、温态、热态和极热态 4 种启动工况下的热应力进行了仿真计算, 并与常物性

下热应力的结果进行了比较, 分析两种结果偏差产生的原因, 以期为准确掌握汽轮机转子的热应力水平提供参考。

## 1 热应力计算模型

### 1.1 温度场的计算

600 MW 汽轮机转子是一个无中心孔的二维轴对称体, 考虑到其轴向热流密度甚微, 所以计算时认为转子是一个处于非稳态条件下各向同性且无内热源的一维无限长圆柱体模型, 这样简化处理后使得模型计算简单、准确可靠<sup>[1,8]</sup>, 适用于工程上的在线计算需要, 其数学模型及边界条件为:

$$\begin{cases} \frac{\partial t(R, \tau)}{\partial \tau} = a \left( \frac{\partial^2 t(R, \tau)}{\partial R^2} + \frac{1}{R} \frac{\partial t(R, \tau)}{\partial R} \right) \\ t(R, 0) = t_0 \\ \frac{\partial t(R, \tau)}{\partial R} \Big|_{R=0} = 0 \\ \frac{\partial t(R, \tau)}{\partial R} \Big|_{R=R_2} = -\frac{\alpha}{\lambda} (t - t_s) \end{cases} \quad (1)$$

式中:  $t$ —转子温度;  $R$ —转子任一点的半径;  $\tau$ —时间;  $a$ —热扩散率;  $\alpha$ —蒸汽与转子表面间的换热系数;  $t_s$ —与转子外表面接触的蒸汽温度;  $R_2$ —转子外径;  $\lambda$ —转子材料的导热系数。

采用克兰克-尼科尔森差分法代替式(1), 得:  
内部节点方程:

$$\frac{t'_i - t_i}{\Delta \tau} = a \left[ \frac{1}{2} \left( \frac{t'_{i-1} - 2t'_i + t'_{i+1}}{\Delta R^2} + \frac{t_{i-1} - 2t_i + t_{i+1}}{\Delta R^2} \right) + \frac{1}{2R_i} \left( \frac{t_i - t_{i-1}}{\Delta R} + \frac{t'_i - t'_{i-1}}{\Delta R} \right) \right] \quad (2)$$

中心节点方程:

$$\left( F_0 \frac{\Delta R}{2} + \frac{\Delta R}{4} \right) t'_i - F_0 \frac{\Delta R}{2} t'_2 = F_0 \frac{\Delta R}{2} (t_2 - t_1) + t_1 \frac{\Delta R}{4} \quad (3)$$

外表面节点方程:

$$F_o(R_n - \frac{\Delta R}{2})t'_{n-1} - [F_o(R_n - \frac{\Delta R}{2}) + R_n - \frac{\Delta R}{4}]t'_n = -F_o(R_n - \frac{\Delta R}{2})(t_{n-1} - t_n) - (R_n - \frac{\Delta R}{4}) \times t_n + \frac{2F_o \alpha R_n \Delta R (t_n - t_s)}{\lambda} \quad (4)$$

式中:  $t'_i$ —下一时刻节点  $i$  的温度值;  $t_i, t_{i-1}$ —该时刻节点  $i$ 、节点  $i-1$  的温度值;  $\Delta\tau$ —时间间隔;  $R_i$ —节点  $i$  处的半径;  $\Delta R$ —分层厚度;  $F_o = \frac{\alpha \Delta\tau}{(\Delta R)^2}$ —傅立叶数。

### 1.2 热应力的计算

$$\sigma_{th} = sK_{th}(t_{ave} - t) \quad (5)$$

式中:  $s = \frac{E\beta}{1-\nu}$ —热应力系数;  $K_{th}$ —应力集中系数;  $t_{ave} = \frac{2}{R_2} \int_0^{R_2} tRdR$ —转子体积平均温度;  $t$ —转子外表面温度。

## 2 转子材料的变物性处理

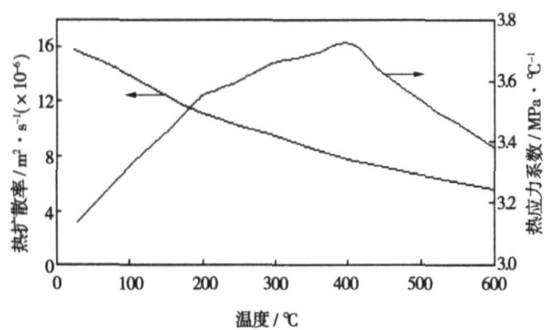


图 1 转子材料热扩散率、热应力系数随温度变化曲线

在机组启停或负荷变动时, 转子温度是个瞬态变化量, 因此必须对转子材料作变物性处理, 以体现任意时刻材料各项物理性质的变化。为计入这种变物性的影响, 归纳于热扩散率  $a = \lambda / \rho c$  与热应力系数  $s = E\beta / (1 - \nu)$  的变化, 将这些不同温度下的数据值, 采用最小二乘法拟合处理, 得到  $a = f(t)$ 、 $s = \varphi(t)$ , 这里  $t$  为转子的体积平均温度, 将其函数关系绘制成曲线图, 如图 1 所示。

由图 1 可以看出: 热扩散率随温度升高而减小, 基本上呈线性变化; 而热应力系数基本分段呈线性变化, 当温度达到 400 °C 时, 其值最大。

## 3 计算对象

汽轮机型号是 CLN600-24.2/566/566-1, 超临界、一次中间再热、单轴、三缸、四排汽, 反动凝汽式汽轮机。高中压转子是无中心孔合金钢整锻转子, 转子材料为: 30Cr1Mo1V 耐热合金钢。

通常在汽轮机高、中压转子的前轴封段和前几级, 在启停及负荷变动的过程中, 汽温的变化最为剧烈, 导致该部位的温度梯度及热应力最大, 成为整个转子的最危险部位, 所以这里选取该机型下的高压段调节级根部光轴截面作为监测对象, 该截面直径为: 0.436 m, 将其沿径向分为 12 层进行计算。

## 4 仿真试验及结果分析

就以上选取的计算对象, 分别取转子初始温度为 130、280、420 和 520 °C, 按照某电厂超临界汽轮机标准的冷态、温态、热态和极热态启动工况进行了仿真试验。图 2 表示了其冷态启动过程中各参数的变化情况, 图 3~图 6 分别表示了在该 4 种启动过程中所得的热应力变化曲线。

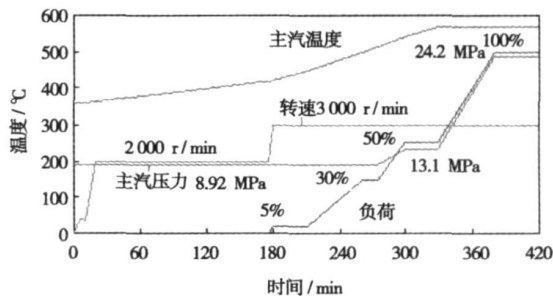


图 2 冷态启动过程中各参数变化曲线

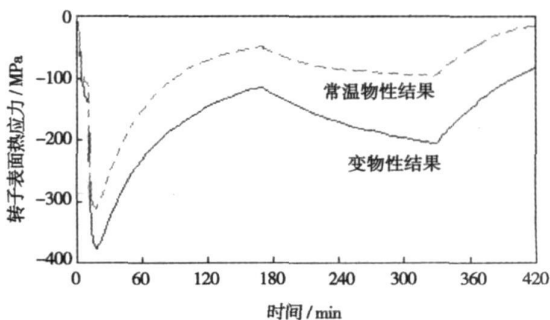


图 3 冷态启动过程中热应力的变化曲线

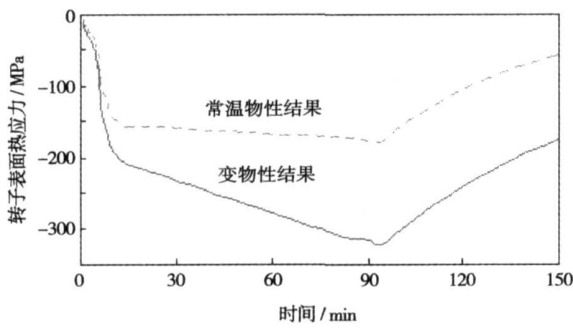


图 4 温态启动过程中热应力的变化曲线

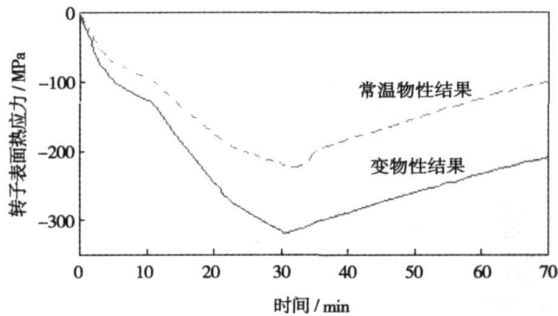


图 5 热态启动过程中热应力的变化曲线

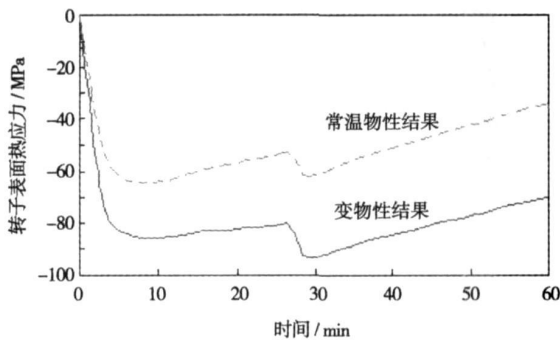


图 6 极热态启动过程中热应力的变化曲线

从图中可以看出:在 4 种启动工况下,考虑材料物性随温度变化的热应力结果均大于常物性下的结果。这是由于在热应力计算中,热应力系数与热应力成正比例关系;而热扩散率越小,转子的导热能力越差,这样导致转子内外温差加大,所以热应力也越大。这种偏差在启动初期较小,但随着启动的深入偏差越来越明显,最高甚至可以达到 2~3 倍。这是由于启动初期材料的工作温度较低,热扩散率较大而热应力系数较小,所以对热应力的影响较小,但随着启动的逐渐深入,转子的的工作温度逐渐升高,这种影响也就越显著。表 1 列出了 4 种启动工况下采

用变物性和常物性计算的最大热应力值及其偏差。由此可见,未考虑材料物性变化的影响会给热应力的准确计算带来较大的误差。

表 1 变物性和常温物性下 4 种启动的最大热应力值及其偏差

	最大热应力值/MPa			
	冷态启动	温态启动	热态启动	极热态启动
变物性	-376.138	-322.322	-319.860	-93.438
常物性	-311.878	-177.812	-221.331	-61.592
偏差	64.26	144.51	98.529	31.846

## 5 结 论

所建转子热应力计算模型,考虑了转子材料物性随温度变化的影响。通过仿真试验,分析了国产某 600 MW 超临界汽轮机冷态、温态、热态和极热态 4 种启动工况下转子热应力的变化趋势,并与常物性转子热应力模型的计算结果进行了比较。结果表明,转子材料物性参数随温度的变化显著影响其启动热应力的大小,材料的变物性影响是不容忽视的。如果转子热应力计算模型忽略材料物性参数的变化,其计算结果将存在较大的误差。本文的研究结果,可为提高汽轮机转子热应力在线监测模型的计算精度提供有益参考。

## 参考文献:

- [1] 支小牧,寇可新,曹向秋. 汽轮机转子热应力在线监测、寿命管理及优化启停的研究[J]. 动力工程, 2001, 20(1): 543-547.
- [2] 张恒良,谢诞梅,熊扬恒等. 600 MW 汽轮机转子高精度热应力在线监测模型研制[J]. 中国电机工程学报, 2006 26(1): 21-25.
- [3] 毛雪平,刘宗德,杨 昆等. 30CrMoV 转子钢高温下的低周疲劳特性试验研究[J]. 中国电机工程学报, 2002, 22(6): 119-122.
- [4] ANDRZEJ G K. The influence of start-ups and cyclic loads of steam turbines conducted according to European standards on the component's life[J]. The Silesian University of Technology, Energy, 2001, 26: 1083-1099.
- [5] MEETHAM G W. Steel and nickel alloys at high temperatures; part D of the requirements for and limitations of materials at high temperatures [J]. Materials & Design, 1989, 10(2): 77-92.
- [6] 王从曾. 材料性能学[M]. 北京: 北京工业大学出版社, 2001.
- [7] 陶曾毅. 电厂金属材料[M]. 北京: 水利水电出版社, 1986.
- [8] 李爱军,谢诞梅,杨 俊,等. 国产 200 MW 汽轮机转子在线热应力监测与寿命管理[J]. 热能动力工程, 2001, 16(1): 86-88.
- [9] ZUCCA S, BOTTO D, GOIA M M. Faster on-line calculation of thermal stresses by time integration[J]. International Journal of Pressure Vessels and Piping, 2004, 81: 393-399.
- [10] ERCAN ATAER O. An approximate method for transient behavior of finned-tube cross-flow heat exchangers[J]. International Journal of Refrigeration, 2004, 27: 529-539.

(编辑 伟)

process, Numeca/design 3D software was used. By an optimized joint employment of an artificial neural network and a genetic algorithm, the general performance can be enhanced by way of an increase in localized performance. The flow field thus involved was calculated by seeking a solution for the full three-dimensional viscous flow N-S equation. Moreover, the authors have verified the feasibility of the method under discussion with a three-stage turbine and a four-stage one serving as examples. **Key words:** turbo-machinery, multi-stage turbine, aerodynamic optimization design, quasi three-dimensional design, design flow path, genetic algorithm, artificial neural network

**涡轮静叶栅二次流的数值模拟 = A Study of the Numerical Simulation of Secondary Flows in Turbine Stator Cascades** [刊, 汉] / LI Jun, SU Ming (Education Ministry Key Laboratory on Turbo-machinery and Engineering, Shanghai Jiaotong University, Shanghai, China, Post Code: 200030) // Journal of Engineering for Thermal Energy & Power. — 2008, 23(1). — 16 ~ 20

By adopting CFD (computational fluid dynamics) Software Fluent a numerical solution for the three-dimensional flows in turbine stator cascades featuring a big turning angle has been achieved. The secondary flows along the flow direction on various sections of the cascade and its aerodynamic characteristics were analyzed along with an investigation of the influence of any change in blade height and inlet incidence on cascade secondary flows. It has been found from the calculation results that the intensity of the secondary flows, which move from the cascade pressure surface to the suction one, increases gradually along the flow direction, giving rise to the continuous consolidation of the boundary layer on endwall near the suction surface and also a curling-up at the rear portion. Moreover, the foregoing also has led to a drastic change of the total pressure loss coefficient and the outlet flow angle along the blade height. A comparison of the various cascade operating conditions shows that a decrease of blade height and an increase of incidence will drastically increase the cascade secondary-flow losses, the intrinsic cause of which invariably lies in the expansion of the area occupied by the secondary flows in the cascade passage. **Key words:** secondary flow, turbine, stator cascade, numerical simulation

**转子物性对超临界汽轮机启动热应力的影响 = The Influence of Rotor Physical Property on Thermal Stresses in a Supercritical Steam Turbine during its Startup** [刊, 汉] / LIU Yan-feng, HAO Run-tian, GAO Jian-qiang, et al (College of Energy Source and Power Engineering, North China Electric Power University, Baoding, China, Post Code: 071003) // Journal of Engineering for Thermal Energy & Power. — 2008, 23(1). — 21 ~ 23

In most cases steam turbine rotors are made of 30CrMoV low carbon alloy steel, the physical property parameters of which change significantly with temperature. The model established for calculating rotor thermal stresses has taken into account the influence of the temperature-dependent change of rotor-material physical property. Through a simulation test, analyzed was the variation tendency of rotor thermal stresses in a domestically-made 600 MW supercritical steam turbine under the following four start-up operating conditions, namely, cold-state, warm-state, hot-state and extremely-hot-state. Moreover, the tendency in question was compared with that obtained from a thermal-stress model featuring a rotor of constant physical property. It has been shown that the change of rotor material physical parameters with temperature will significantly influence the magnitude of the start-up thermal stresses. The above finding can provide a helpful reference for enhancing the calculation accuracy of an on-line monitoring model involving turbine-rotor thermal stresses. **Key words:** steam turbine rotor, physical property, thermal stress, model

**凝汽器运行状态的物元模型及可拓评价方法 = An Object-element Model for Depicting the Operating States of a Condenser and its Extensible Evaluation Method** [刊, 汉] / LU Xu-xiang, LI Lu-ping (College of Energy Source and Power Engineering, Changsha University of Science and Technology, Changsha, China, Post Code: 410076) // Journal of Engineering for Thermal Energy & Power. — 2008, 23(1). — 24 ~ 27

On the basis of establishing indexes for evaluation of the operating states of condensers, presented was an extensible method for the above evaluation in the light of diversity and fuzziness of the evaluation indexes. The proposed method was based on an object-element model and extensible correlation functions. In combination with currently available literature